

Mobility gap in intermediate valent TmSe

M. DUMM¹, B. GORSHUNOV^{1,2}, M. DRESSEL¹ and T. MATSUMURA³

¹ *1. Physikalisches Institut, Universität Stuttgart, Pfaffenwaldring 57, 70550 Stuttgart, Germany*

² *General Physics Institute, Moscow, Russia*

³ *Department of Physics, Graduate School of Science, Tohoku University, Sendai 980-8578, Japan*

PACS. 71.28.+d – Narrow-band systems; intermediate-valence solids.

PACS. 75.30.Mb – Valence fluctuation, Kondo lattice, and heavy-fermion phenomena.

Abstract. – The infrared optical conductivity of intermediate valence compound TmSe reveals clear signatures for hybridization of light d - and heavy f -electronic states with $m^* \approx 1.6m_0$ and $m^* \approx 16m_0$, respectively. At moderate and high temperatures, the metal-like character of the heavy carriers dominate the low-frequency response while at low temperatures ($T_N < T < 100K$) a gap-like feature is observed in the conductivity spectra below 10 meV which is assigned to be a mobility gap due to localization of electrons on local Kondo singlets, rather than a hybridization gap in the density of states.

Introduction. – Among the intermediate valence semiconductors, TmSe attracts particular interest because of its unique characteristics [1, 2]. Unlike other members of the family, both valence states of the rare earth counterpart, Tm^{2+} and Tm^{3+} (the mean valence of Tm ion is +2.75 [1]), carry magnetic moments [2]. Below the Néel temperature $T_N = 3.5$ K, TmSe reveals a long-range ordered antiferromagnetic phase with strongly pressure and magnetic field dependent properties [3]. These peculiarities are considered to be the reason for a variety of unusual transport, optical and magnetic properties of this intermediate valence compound, like the magnetic field, temperature and pressure dependence of the resistivity and Hall effect [4, 5], anisotropy of magnetization and magnetostriction [6], temperature and pressure dependence of quasi-elastic absorption in the neutron scattering experiments [7], complicated structure of the optical spectra in the low-energy region of a few meV [2, 8] and the origin of the insulating antiferromagnetic state below T_N [1, 2, 9]. All of these properties are likely to be related to the microscopic mechanism of the valence fluctuations in TmSe which are under intensive study. It should be noted, however, that to a significant extent the attention is focused on the study of the magnetically ordered phase at $T < T_N$. At the same time also at higher temperatures, up to the room temperature, TmSe reveals a behavior which is not completely understood. For instance, the dc resistivity $\rho(T)$ is increasing towards liquid helium temperatures by about an order of magnitude starting with 300 K and it does not show any sign of an activated behavior as other mixed valence compounds do, like YbB_{12} [10, 11] or SmB_6 [12, 13], where the opening of a hybridization gap governs the resistivity behavior.

The same is true for the Hall measurements [4, 9, 14]. It is assumed that the Kondo scattering on the localized f -spins is responsible for the temperature variation of resistivity and Hall constant [4, 15], however, the correspondent $\rho(T) \propto -\log T$ behavior is observed only in a narrow temperature range between 4 K to 40 K [9]. The magnetic susceptibility follows the Curie-Weiss law starting from 300 K down to 35 K [9]. Below this temperature the magnetic moment of the Tm ions is enhanced, contrary to other mixed valence semiconductors.

In earlier optical studies, a typical metallic reflectivity plasma edge was observed at energies of a few eV [2, 8]. At lower energies signatures of a non-Drude-like behavior were seen already at room temperature [8]. The optical properties were also investigated in the antiferromagnetic ground state [2]. However, up to now there exists no study of the temperature dependent evolution of the infrared spectra in the paramagnetic phase. Here, we present a detailed investigation of TmSe at temperatures 5 K to 300 K by means of far-infrared spectroscopic and dc resistivity measurements. The aim of the present work was a comprehensive study of the charge carrier dynamical properties in TmSe in the paramagnetic phase. All experiments were performed in zero magnetic field.

Experiment and results. – We used high quality single crystals grown as described in [16]. The typical size of the copper red single crystals used for the optical experiments was 2 by 2 mm². Reflectivity spectra were measured at nearly normal incidence employing a Bruker IFS 113v spectrometer in the frequency range $20 \text{ cm}^{-1} < \nu < 10000 \text{ cm}^{-1}$ at temperatures $5 \text{ K} < T < 300 \text{ K}$. Reference spectra for calculating absolute values of reflectivity were recorded using the in-situ Au-coating technique [17]. In addition, quasi-optical reflectivity measurements [18] were performed down to lowest frequencies $\nu = 10 \text{ cm}^{-1}$. From the frequency dependent reflectivity we derived the real part of the optical conductivity σ_1 and the permittivity ϵ_1 by Kramers-Kronig analysis. We used our dc resistivity data for the low-frequency extrapolation and previously published data [8] for the high frequency extrapolation. The dc resistivity was measured using standard four-probe technique.

At all temperatures, the reflectivity of TmSe is high as usually observed in conductors. The spectra of conductivity and permittivity of TmSe derived from the recorded reflectivity data are shown in fig. 1 for several temperatures. At frequencies above approximately 1000 cm^{-1} the present results are the same as reported previously at $T = 3.5 \text{ K}$ and 300 K [2, 8]. The spectra of conductivity and dielectric constant are Drude-like and almost temperature independent in the mid- and near-infrared frequency region with a characteristic roll-off around the scattering rate γ . Fits of $\sigma(\nu)$ and $\epsilon(\nu)$ by the Drude model [19] yield $\gamma = 4700 \text{ cm}^{-1}$ and the plasma frequency $\nu_p = 38500 \text{ cm}^{-1}$ of the conduction carriers; the corresponding plasma energy of 4.8 eV agrees with the data given in [8].

However, strong deviations from the Drude behavior are observed at low frequencies, particularly below 100 cm^{-1} . At 300 K, an additional bump is found in the conductivity spectrum in this frequency region, coming along with a correspondent dispersion of the permittivity. When cooling down to $T = 200 \text{ K}$, the spectra do not change significantly. At even lower temperatures, however, the low-frequency bump loses its strength and diminishes; the reflectivity starts to decrease gradually. Cooling below 50 K, the bump in $\sigma(\nu)$ turns into a gap-like feature. The spectra do not change any further between $T = 20 \text{ K}$ and 5 K . Correspondingly, at low temperatures the permittivity is as large as $\epsilon_1 = 4500$ below $\nu = 20 \text{ cm}^{-1}$.

The temperature dependent resistivity (fig. 2) is in accord with the optical data and previously reported results [4, 9, 20]. There is a very small increase of $\rho(T)$ when cooling from 300 K to 200 K. Below about 100 K, the resistance rises stronger and follows a Kondo-type behavior $\rho(T) \propto -\log T$ between $T = 35 \text{ K}$ and the Néel temperature T_N [9]; hence the Kondo temperature is estimated to be $T_K \approx 40 \text{ K}$ [21]. Below 4 K $\rho(T)$ seems to saturate, but a sharp

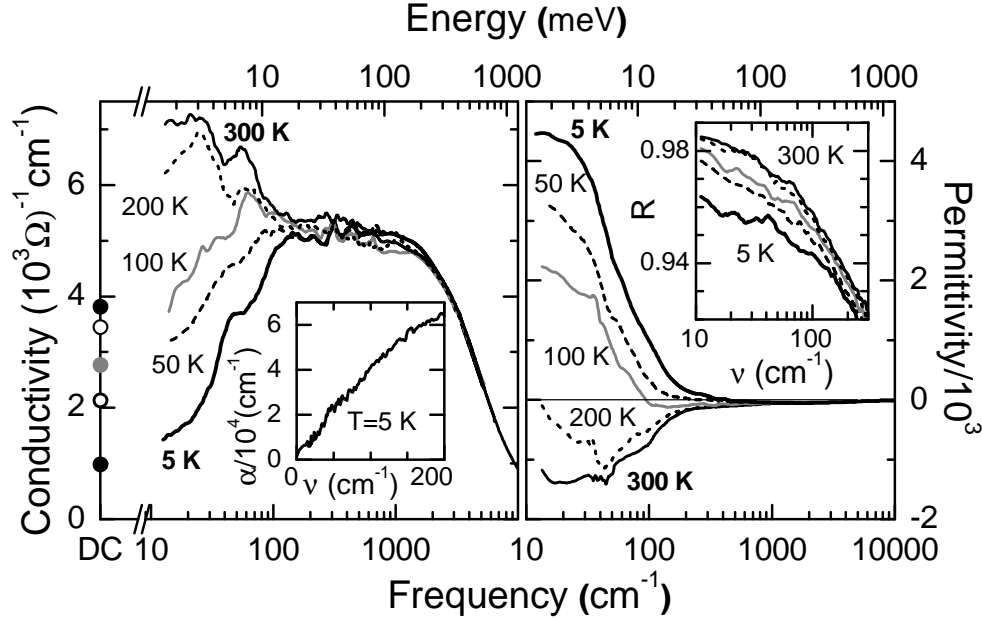


Fig. 1 – Spectra of optical conductivity and permittivity of TmSe at different temperatures as indicated. The symbols on the conductivity ordinate represent the corresponding dc values. In the insets the absorption coefficient α at 5 K (left panel) and the reflectivity R (right panel) are shown. The temperatures for the σ_{dc} and R data are from top to bottom 300 K, 200 K, 100K, 50 K, 5 K.

kink followed by a step increase is observed below $T_N = 3.5$ K when the system enters the antiferromagnetic phase [9]. Similar to [8], the dc conductivity σ_{dc} is noticeably lower than the far-infrared values at elevated temperatures ($T = 300$ K and 200 K), while the difference diminishes below 50 K.

Discussion. – The charge dynamics of TmSe has been subject of discussion since the transport characteristics like resistivity and Hall constant are not thermally activated [2,4,9,22] and no low-temperature decrease of magnetic susceptibility was reported [9,23]. These findings are in contrast to intermediate-valence compounds with even number of electrons per unit cell like YbB₁₂ and SmB₆. Here, signatures of thermally activated behavior are observed in resistivity [10,12], Hall [10,13] and optical conductivity [24] which is in agreement with an opening of a hybridization gap at the Fermi level in the density of states upon cooling [2]. The gap-like feature observed at low temperatures in our optical spectra of TmSe, however, cannot be connected to a hybridization gap in the density of states for the following reasons:

(i) TmSe is an odd-number electron system for $T > T_N$ which should not exhibit a hybridization gap at E_F according to the Luttinger theorem [25]. Only in the antiferromagnetically ordered phase the hybridization gap is ‘allowed’, since the magnetic unit cell doubles and therefore hosts an even number of f and d electrons. Indeed, a gap of $\Delta_{hyb} \approx 1 - 2$ meV was observed for $T < T_N$ [2,26]. The periodic Anderson model which has been treated with dynamical mean-field theory predicts that the hybridization gap is expected to form below $T^* = \Delta_{hyb}/5$ [27]. Interestingly, in TmSe T^* coincides with T_N .

(ii) As seen from the inset of fig. 1, the absorption coefficient $\alpha = 2k\omega/c$ (k is the extinction

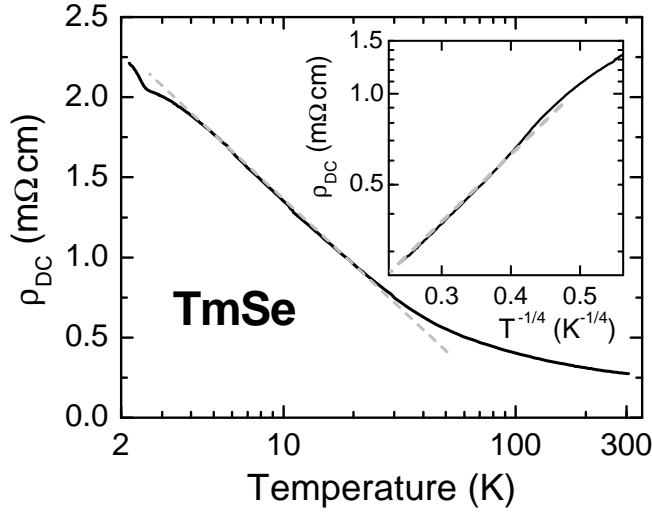


Fig. 2 – Temperature dependence of the dc resistivity of TmSe. The dashed line shows a Kondo behavior $\rho(T) \propto -\log T$ above the Néel temperature $T_N = 3.5$ K and below the Kondo temperature $T_K = 40$ K. The inset exhibits the resistivity $\rho(T)$ vs $T^{-1/4}$; this temperature dependence indicates variable-range hopping in the range $T = 40 - 300$ K.

coefficient and c the speed of the light) smoothly approaches zero as $\nu \rightarrow 0$ and does not reveal an absorption-edge structure, as observed in semiconductors with a gap in their density of states [29].

(iii) The resistivity is not thermally activated, instead it shows a $\rho \propto -\log T$ dependence.

Therefore, we can conclude that at $T > T_N$ the charge dynamics is dominated by inelastic Kondo scattering. In this case, the Kondo lattice system TmSe behaves analogously to a dilute Kondo system. The density of electronic states of such a system is displayed in the inset of fig. 3. The bottom of the $5d$ conduction band overlaps the occupied $4f^{13}$ level of Tm^{2+} where the electrons are localized. As a result a hybridized $4f^{13}-4f^{12}5d$ state evolves at the Fermi level E_F , and the combined quasiparticle density of states reveals a Kondo peak of width W at E_F . No hybridization gap is present at E_F due to the reasons given above.

The optical and resistivity data can now be interpreted based on this scheme. The density of states exhibits a peak at E_F well above the Kondo temperature, even at room temperature; this fact was also observed for other heavy fermion and intermediate valence compounds [2,30]. Due to hybridization the electrons in the vicinity of the Fermi level have both d as well as f character. They contribute to the optical response if the electromagnetic radiation probes the region of enhanced density of states inside the Kondo peak. Thus, the enhanced conductivity and negative permittivity below 100 cm^{-1} (fig. 1) at moderate temperatures $T = 200 - 300$ K indicate the formation of a Kondo peak already at such high temperatures.

For a more detailed analysis of the frequency dependence of the optical data we introduce a frequency dependent quasi-particle scattering rate $\tau^{-1}(\omega)$ and effective mass $m^*(\omega)$. Now, the low-frequency resonance is attributed to the renormalization of $\tau^{-1}(\omega)$ and $m^*(\omega)$. Such an analysis is widely applied for highly correlated electron systems since it uses just one type of charge carriers and therefore does not require to arbitrarily separate the response into different components [31]. The renormalization is quantified within the generalized Drude model where

a complex scattering rate $\hat{\Gamma}(\omega) = \tau^{-1}(\omega) - i\omega\lambda(\omega)$ is introduced into the standard Drude formula:

$$\sigma_1(\omega) = \frac{(\omega_p)^2}{4\pi} \frac{1}{\hat{\Gamma}(\omega) - i\omega} = \frac{(\omega_p)^2}{4\pi} \frac{1}{\tau^{-1}(\omega) - i\omega(m^*(\omega)/m)} \quad (1)$$

$\lambda(\omega)$ relates the frequency dependent effective mass $m^*(\omega)/m = 1 + \lambda(\omega)$ to the frequency dependence of the effective scattering rate $\tau^{-1}(\omega)$ which are both linked by the Kramers-Kronig integrals [19]. By rearranging eq. (1), expressions for $\tau^{-1}(\omega)$ and $m^*(\omega)$ in terms of real and imaginary parts of the conductivity, $\sigma_1(\omega)$ and $\sigma_2(\omega) = \omega\epsilon_1/(4\pi)$, are obtained:

$$\tau^{-1}(\omega) = \frac{(\omega_p)^2}{4\pi} \frac{\sigma_1(\omega)}{|\hat{\sigma}(\omega)|^2}, \quad \frac{m^*(\omega)}{m} = \frac{(\omega_p)^2}{4\pi} \frac{\sigma_2(\omega)}{|\hat{\sigma}(\omega)|^2} \frac{1}{\omega}. \quad (2)$$

Fig. 3 shows the calculated frequency dependences of effective quasiparticles scattering rate $\gamma(\nu) = \tau^{-1}(\nu)/(2\pi c)$ and effective mass $m^*(\nu)/m_b$ where m_b is the band mass and $\nu = \omega/(2\pi c)$. At high frequencies the electrons in the conduction band dominate with a scattering rate $\gamma \approx 4200 \text{ cm}^{-1}$, a value which is comparable to the one obtained from the simple Drude fit (see above and fig. 1). For frequencies below approximately 200 cm^{-1} , the effective scattering rate decreases which indicates the reduced scattering due to the admixture of heavy f electrons. The effective mass obtained at high frequencies is close to the band mass, $m^* \approx m_b$, which is about 1.6 times the free electron mass m_0 [8]. Going to lower frequencies, it grows up to $m^* \approx 10m_b \approx 16m_0$; this is an indication of hybridization effects and of the presence of the Kondo peak at the Fermi level already at room temperature. This peak in the density of states should have no influence on the optical response for frequencies considerably larger than its width, $h\nu \gg W$. Since no significant temperature dependence is observed in the optical spectra above 100 cm^{-1} , the width W of the Kondo peak in TmSe can be estimated from our optical data to be around 10 meV at room temperature. The Kondo temperature $T_K = 40 \text{ K}$ obtained from the dc resistivity provides an estimation for W at

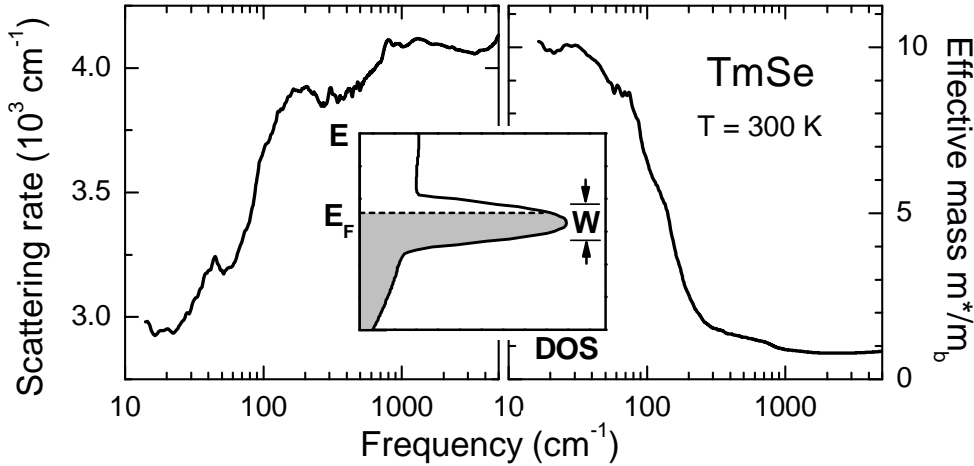


Fig. 3 – Frequency dependence of effective scattering rate $\gamma(\nu)$ and effective mass $m^*(\nu)$ in TmSe at ambient temperatures. The inset schematically shows the quasi-particle density of states for a Kondo lattice system with odd number of f and d electrons above the coherence temperature T^* with the Kondo resonance of width W at the Fermi level (after [28]).

low temperatures via the relation $W \approx k_B T_K = 3.4$ meV [32]. In agreement with theoretical calculations [27], there is significant broadening of the Kondo peak at temperatures $T \gg T_K$.

When the temperature is lowered, the Fermi function becomes sharper around E_F and consequently the admixture of f -type carriers grows. For $T < T_K$ this leads to a logarithmic increase of the resistivity as displayed in fig. 2, and which is characteristic for incoherent Kondo scattering. The consequence is a reduced low-energy spectral weight in the conductivity spectrum which resembles a gap-like feature. Now it becomes clear that this feature is a mobility gap [33] and should be associated with the energy needed to delocalize the charge carriers bound to local Kondo singlets. As discussed above, the real hybridization gap will only develop in the magnetically ordered phase below $T_N = 3.5$ K. Its measured value of $\Delta_{\text{hybr.}} \approx 1 - 2$ meV is considerably smaller than the gap-like depression present in our far-infrared conductivity data. It is not intended to quantitatively analyze our data in detail. The behavior observed in the optical spectra of TmSe at low frequencies is in qualitative agreement with results obtained by simple early models [2, 8, 34] and more rigorous models [31, 35], also including the magnetic field dependences of the TmSe transport properties.

Finally, a brief comment on the relation between σ_{dc} and far-infrared response. At low temperatures, the optical conductivity can be smoothly extrapolated into the dc limit. Here, both dc and ac responses are determined by the heavy f -electron component since for $T < 50$ K the thermal energy $k_B T$ is in the order of the width W of the Kondo peak. Contrary, as seen in fig. 1, at high temperatures there is an obvious mismatch between both data sets: for $T = 300$ K and 200 K, where the reflectivity is extremely high in the low-frequency limit, $\sigma_1(\nu)$ shows clear signatures of metallic Drude-like behavior above $\nu = 10$ cm $^{-1}$, i.e., the conductivity decreases with increasing frequency. However, in order to match the dc data, $\sigma_1(\nu)$ has to decrease by a factor of two below $\nu = 10$ cm $^{-1}$; an observation which is in accordance with previously reported results at 300 K [8]. As shown in the inset of fig. 2, from 40 K up to 300 K the dc resistivity follows the behavior $\rho(T) = \rho(0) \exp[T_0/T]^{1/4}$ which is characteristic for the variable range hopping [33] in systems with localization. According to Mott [33], the low-frequency conductivity in this regime shows a behavior of the type $\sigma_1(\nu, T) = \sigma_{\text{dc}}(T) + \sigma_0 \nu^s$ with an exponent $s \approx 1$ and the constant σ_0 , which is frequently observed in disordered materials at radio frequencies [36]. Also for TmSe the frequency dependent transport is expected to follow this behavior which is, however, restricted to frequencies well below $\nu = 10$ cm $^{-1}$ and therefore explains the mismatch of dc and ac data in fig. 1.

Conclusions. – The optical spectra of conductivity and permittivity of the intermediate valence compound TmSe have been measured down to low frequencies ($\nu \approx 10$ cm $^{-1}$) at temperatures 5 - 300 K, i.e. in the paramagnetic state. At high temperatures, the Drude-like mid-infrared conductivity is associated with the d electrons in the conduction band which have a plasma energy of 4.8 eV and an effective mass close to free electron mass m_0 while the enhanced very far-infrared conductivity is connected with an admixture of f electrons to the charge-carrier condensate as a result of the hybridization of itinerant d and localized f electrons. These carriers are characterized by a reduced scattering rate γ and an enhanced effective mass of $m^* \approx 16m_0$ at around room temperatures, indicating correlation effects. At low temperatures, 5 K $< T < 50$ K, a gap-like feature is observed in the conductivity spectra for frequencies $\nu < 100$ cm $^{-1}$ which is accounted for as a mobility gap due to localization of d electrons on local Kondo singlets.

We are grateful to D. Faltermeier and P. Haas for their experimental support. The project

was supported by the Deutsche Forschungsgemeinschaft (DFG) and the program for fundamental research of the Division of Physical Sciences, RAS, "Problems of Radiophysics".

REFERENCES

- [1] BUCHER E. *et al.*, *Phys. Rev. B*, **11** (1975) 500.
- [2] WACHTER P., *Handbook on the Physics and Chemistry of Rare Earths*, edited by GSCHNEIDER, K. A. JR. *et al.*, Vol. **19** (North-Holland, Amsterdam) 1994, p. 177.
- [3] GUERTIN R. P., FONER S. and MISSELL F. P., *Phys. Rev. Lett.*, **37** (1976) 529; BJERRUM MØLLER H., SHAPIRO S. M. and BIRGENEAU R. J., *Phys. Rev. Lett.*, **39** (1977) 1021.
- [4] CLAYMAN B. P., WARD R. W. and TIDMAN J. P., *Phys. Rev. B*, **16** (1977) 3734.
- [5] RIBAUT M. *et al.*, *Phys. Rev. Lett.*, **45** (1980) 1295; OHASHI M. *et al.*, *Physica B*, **259-261** (1999) 326.
- [6] NAKANISHI Y. *et al.*, *Physica B*, **281-282** (2000) 595.
- [7] MIGNOT J.-M. *et al.*, *Physica B*, **276-278** (2000) 756; SCHLOTTMANN P., *Phys. Rev. B*, **29** (1984) 630; SHAPIRO S. M. and GRIER B. H., *Phys. Rev. B*, **25** (1982) 1457.
- [8] BATLOGG B., *Phys. Rev. B*, **23** (1981) 1827.
- [9] BATLOGG B. *et al.*, *Phys. Rev. B*, **19** (1979) 247.
- [10] KASAYA M. *et al.*, *J. Magn. Magn. Mater.*, **47-48** (1985) 429.
- [11] MOSER M. *et al.*, *Sol. State Commun.*, **54** (1985) 241.
- [12] MENTH A., BUEHLER E. and GEBALLE T. H., *Phys. Rev. Lett.*, **22** (1969) 295.
- [13] ALLEN J. W., BATLOGG B. and WACHTER P., *Phys. Rev. B*, **20** (1979) 4807.
- [14] ANDRES K. *et al.*, *Sol. State Commun.*, **27** (1978) 825.
- [15] HAEN P. *et al.*, *J. Magn. Magn. Mater.*, **63-64** (1987) 603.
- [16] MATSUMURA T. *et al.*, *J. Phys. Soc. Jpn.*, **67** (1998) 612.
- [17] HOMES C. C. *et al.*, *Appl. Optics*, **32** (1992) 2976.
- [18] KOZLOV G.V. and VOLKOV A.A., *Millimeter and Submillimeter Wave Spectroscopy of Solids*, edited by GRÜNER G. (Springer, Berlin) 1998, p. 51.
- [19] DRESSEL M. and GRÜNER G., *Electrodynamics of Solids* (Cambridge University Press, Cambridge) 2002.
- [20] HOLTZBERG F. *et al.*, *J. Appl. Phys.*, **57** (1985) 3152.
- [21] The Kondo temperature T_K usually marks the minimum resistivity which separates the region with $\rho(T) \propto -\log T$ behavior from a metallic temperature dependence of $\rho(T)$ at higher T . Here, it marks the transition from the Kondo behavior to hopping transport around 40 K.
- [22] HAEN P. *et al.*, *J. Magn. Magn. Mater.*, **15-18** (1980) 989.
- [23] HOLTZBERG F., PENNEY T. and TOUNIER R., *J. de Physique*, **40** (1979) 314.
- [24] TRAVAGLINI G. and WACHTER P., *Phys. Rev. B*, **29** (1984) 893; GORSHUNOV B. *et al.*, *Phys. Rev. B*, **59** (1999) 1808; OKAMURA H. *et al.*, *Phys. Rev. B*, **58** (1998) R7496.
- [25] LUTTINGER J. M., *Phys. Rev.*, **119** (1960) 1153; MARTIN R. M. and ALLEN J. W., *J. Appl. Phys.*, **50** (1979) 7561.
- [26] GÜNTHERODT G. *et al.*, *Phys. Rev. Lett.*, **49** (1982) 1030.
- [27] ROZENBERG M. J., KOTLIAR G. and KAJUETER H., *Phys. Rev. B*, **54** (1996) 8452.
- [28] VARMA C. M., *Rev. Mod. Phys.*, **48** (1976) 219.
- [29] MOSS T. S., *Proc. Phys. Soc. B*, **67** (1954) 775.
- [30] BUCHER B. *et al.*, *Phys. Rev. Lett.*, **72** (1994) 522.
- [31] DEGIORGI L., *Rev. Mod. Phys.*, **71** (1999) 687.
- [32] MARTIN R. M., *Phys. Rev. Lett.*, **48** (1982) 362.
- [33] MOTT N. F. and DAVIS E. A., *Electronic Processes in Non-Crystalline Materials*, 2nd edition (Clarendon Press, Oxford) 1979.
- [34] ALLEN J. W. *et al.*, *J. Appl. Phys.*, **49** (1978) 2078.
- [35] ANDERS F. B., JARRELL M. and COX D. L., *Phys. Rev. Lett.*, **78** (1997) 2000.
- [36] DYRE J. C. and SCHRØDER T. B., *Rev. Mod. Phys.*, **72** (2000) 873.